

PAPER • OPEN ACCESS

Estimation of heat dissipation on a levitating rotor over superconducting magnet bearing

To cite this article: T Iida *et al* 2020 *IOP Conf. Ser.: Mater. Sci. Eng.* **755** 012004

View the [article online](#) for updates and enhancements.

You may also like

- [POLICAN: A Near-infrared Imaging Polarimeter at the 2.1m OAGH Telescope](#)
R. Devaraj, A. Luna, L. Carrasco et al.
- [Detection of Polarization due to Cloud Bands in the Nearby Luhman 16 Brown Dwarf Binary](#)
Maxwell A. Millar-Blanchaer, Julien H. Girard, Theodora Karalidi et al.
- [A MEASUREMENT OF THE COSMIC MICROWAVE BACKGROUND *B*-MODE POLARIZATION POWER SPECTRUM AT SUB-DEGREE SCALES WITH POLARBEAR](#)
The Polarbear Collaboration: P. A. R. Ade, Y. Akiba, A. E. Anthony et al.



ECS
The
Electrochemical
Society
Advancing solid state &
electrochemical science & technology

DISCOVER
how sustainability
intersects with
electrochemistry & solid
state science research

Estimation of heat dissipation on a levitating rotor over superconducting magnet bearing

T Iida¹, Y. Sakurai², T Matsumura², H Sugai², H Imada³, H Kataza⁴, H Ohsaki⁵,
N Katayama² and Y Terao⁵

¹ ispace, inc., 2-7-17, Shiba, Minato-ku, Tokyo, 105-0014, JAPAN

² Kavli Institute for the Physics and Mathematics of the Universe (WPI) The University of Tokyo Institute for Advanced Study (UTIAS) The University of Tokyo, 5-1-5 Kashiwanoha, Kashiwa, Chiba 277-8583, JAPAN

³ Laboratoire de l'Accélérateur Linéaire, Université Paris-Sud, Bâtiment 200, 91405 Orsay cedex, France

⁴ Institute of Space and Astronautical Science (ISAS), Japan Aerospace Exploration Agency (JAXA) 3-1-1 Yoshinodai, Chuo, Sagami-hara, Kanagawa 252-5210, JAPAN

⁵ Department of Advanced Energy Graduate School of Frontier Sciences, The University of Tokyo 5-1-5 Kashiwanoha, Kashiwa, Chiba 277-8561, JAPAN

Abstract. We report the estimation of the heat dissipation on a levitating rotor over superconducting magnetic bearing operating below 10 K. The continuously rotating mechanism is one of key devices to support the rotation of a sapphire half wave plate (HWP) in a polarization modulator of a LiteBIRD satellite. Due to the system requirement, the HWP must be kept at a cryogenic temperature while it is spinning. In order to minimize the frictional energy loss, we employ a superconducting magnetic bearing (SMB) and AC synchronous motor, which enables a contactless rotational mechanism. While we can minimize the frictional heat loss, there exists an energy loss due to the magnetic friction. As a result, it is essential to build a thermal model an estimation of heat dissipation to this contactless rotor is important to predict how much the HWP temperature rises during its rotation. For an estimation of heat dissipation, we conduct an experiment in order to establish the thermal simulation model equivalent to the flight model in size. Each thermal contact conductance between the rotor and the cryogenic rotor holder is also estimated through the experiment data. From the data, we only can know the difference in the rotor temperature before and after the rotor rotation. We monitor the transient temperature profile of grippers after the rotor is gripped by them. The rotational time is related to the total heat dissipation on the rotor because the heat dissipation is attributed to two kinds of energy losses: a magnetic hysteresis and induced eddy currents on metal parts of the rotor. Finally, we make a comparison between the thermal model and the experimental result and estimate the allowable heat dissipation to keep the HWP temperature lower than 20K.

1. Introduction

One of the most important research topics in the current cosmology and high-energy particle physics is to study the cosmic inflation, which predicts a rapid expansion of the universe at $\sim 10^{-38}$ seconds after the beginning of the universe [1, 2]. The inflation solves several mysteries of our universe and it can provide a foothold for a new physics microscopically and macroscopically in particle physics and cosmological physics. The cosmic microwave background (CMB) is electromagnetic microwave radiation that contains the information before and after the last scattering surface. The CMB has a



Content from this work may be used under the terms of the [Creative Commons Attribution 3.0 licence](https://creativecommons.org/licenses/by/3.0/). Any further distribution of this work must maintain attribution to the author(s) and the title of the work, journal citation and DOI.

uniform temperature of 2.7 K with a black body spectrum: the CMB is polarized with the amplitude of a few microkelvin fluctuation across the whole sky. There are two types of polarization: one is E-mode and the other is B-mode. E-mode naturally arises from the density perturbations in the early universe. On the other hand, B-mode only originates from primordial gravitational waves by the cosmic inflation. Thus, the CMB polarization contains the fingerprint of the cosmic inflation. In recent years, a world-wide competition toward the first detection is in progress. Correspondingly, the instrumental developments that enable to achieve this science have progressed rapidly.

One of the key instruments for a precise measurement of the CMB polarization is a polarization modulator. It consists of an optical element, a half-wave plate (HWP), and a rotational mechanism. The rotating HWP modulates the CMB polarization signal. The incident signal to the HWP is upconverted in frequency far above the low frequency detector noise.

An ordinary spinning method of the HWP using ball bearings is difficult in a cryogenic environment due to heat dissipation induced by mechanical frictions. Thus, we propose to employ a superconducting magnet bearing (SMB). However, even with a contactless SMB we anticipate the heat dissipation due to magnetic interaction, e.g. hysteresis and eddy current. In this paper, we make an estimation of the heat dissipation from the spinning rotor by constructing the thermal structural model with the experimental data. We also identify the required power in order to maintain the HWP temperature below 20 K.

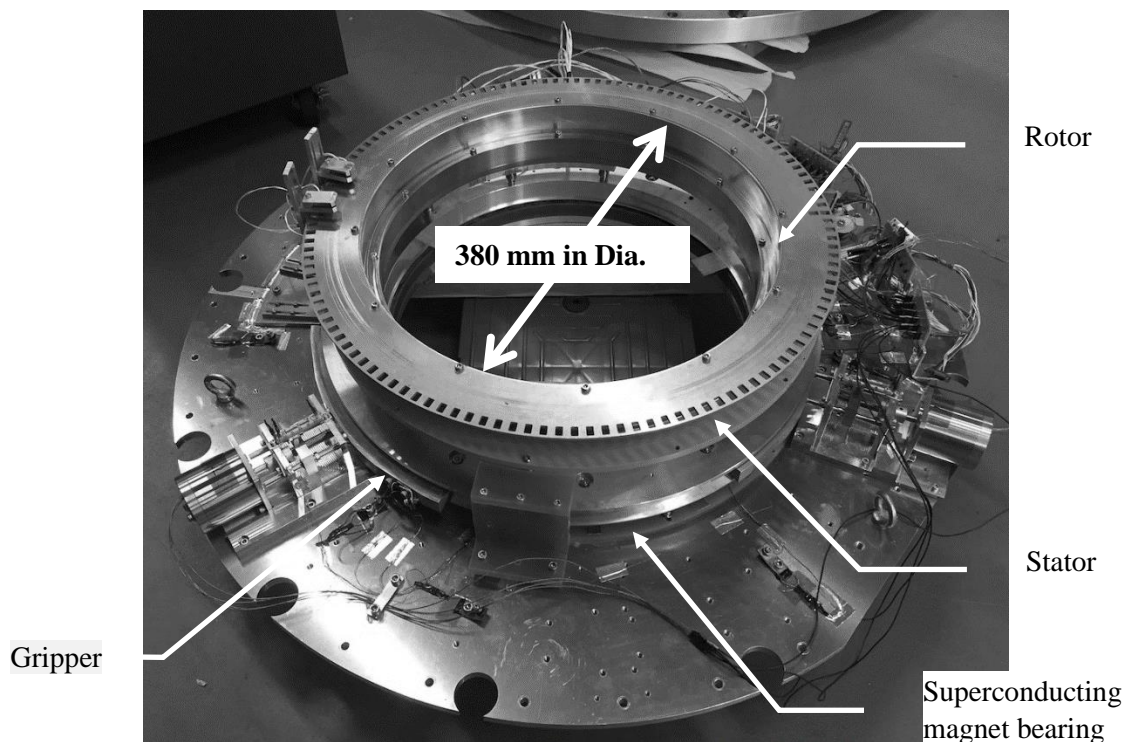


Figure 1. A photo of the breadboard model polarization modulation unit. The HWP are not installed in the photograph.

2. Overview of the polarization modulator unit

A breadboard model of the polarization modulator unit (PMU) is constructed to demonstrate the thermal performance. The entire system, shown in Figure 1, is installed inside of the cryostat. The cryostat is cooled at 4 K using a GM cooler. The PMU consists of a rotor, a stator, a superconducting magnet bearing (SMB) and three grippers.

The rotor has two parts: a rotor top and bottom. The top contains an optical encoder disk and alternatively polarized pairs of Samarium-Cobalt (SmCo) permanent magnets as a part of the drive AC motor. The bottom contains SmCo magnets in a circumferential direction for levitation. The top and

bottom parts are connected by the 6 stainless steel shafts with about 1mm in diameter. The stator contains three parts, an LED and silicon photodiode as a part of the encoder, and drive AC coils. With the AC motor on the rotor top and drive AC coils on the stator, the rotor rotates at an arbitrary rotation speed. The HWP is expected to be mounted at the center of the rotor, but we carried out the test without mounting the HWP. The further detailed description for the system can be found in Sakurai et al. and Matsumura et al. [1, 2].

The SMB is the type-II superconductor of YBCO, which is contained in a G10 chassis. It works as a bearing only below the critical temperature of the YBCO. With the permanent magnet on the rotor bottom and this superconducting magnet, the rotor is levitated over the YBCO magnet. Once the YBCO drops below the critical temperature, the magnetic field from the rotor magnet of the SMB is pinned by the superconductor magnet. The three grippers serve as a holder mechanism. They hold the rotor until the YBCO cools down below the critical temperature. They also provide a conductive thermal path between the gripper and the rotor when it is gripped.

When the rotor rotates at some speed, mainly two types of losses are induced. One is the hysteresis loss and the other is the Joule loss. In both cases, we need the source of the magnetic field inhomogeneity. This source can be originated by the array of the AC motor magnets, the inhomogeneity of the SMB magnet along the circumference, and the inhomogeneity of the trapped magnetic field in the segmented YBCO ring. A part of the energy loss goes to the stator and the rest goes to the rotor. It is best if one can employ a remote sensing cryogenic thermometer [3]. This is rather difficult to achieve with a required accuracy. Another approach is to rely on a thermal-electromagnetic structural model and predict fully how the heat dissipation appears in each component. This approach is in progress, and thus we do not address this approach in this paper.

In this paper, we carry out the estimation of the heat on the rotor given the measurable gripper temperatures when the rotor is stopped and held by the gripper. It is estimated by a temperature sensor mounted on the tip of each gripper arm. We release the rotor for levitation of the rotor over the superconducting magnet, spin it for a certain amount of time, re-grip it and monitor the gripper temperatures. This approach was also demonstrated by the small prototype system [4].

3. Estimation of heat dissipation on rotor and thermal contact conductance of each gripper

3.1 Thermal simulation model

We built a thermal model of the full-size rotor, as shown in Figure 2. The material list for each component is shown in Table 1. The most parts on the rotor are made from aluminium alloy, stainless steel and G10.

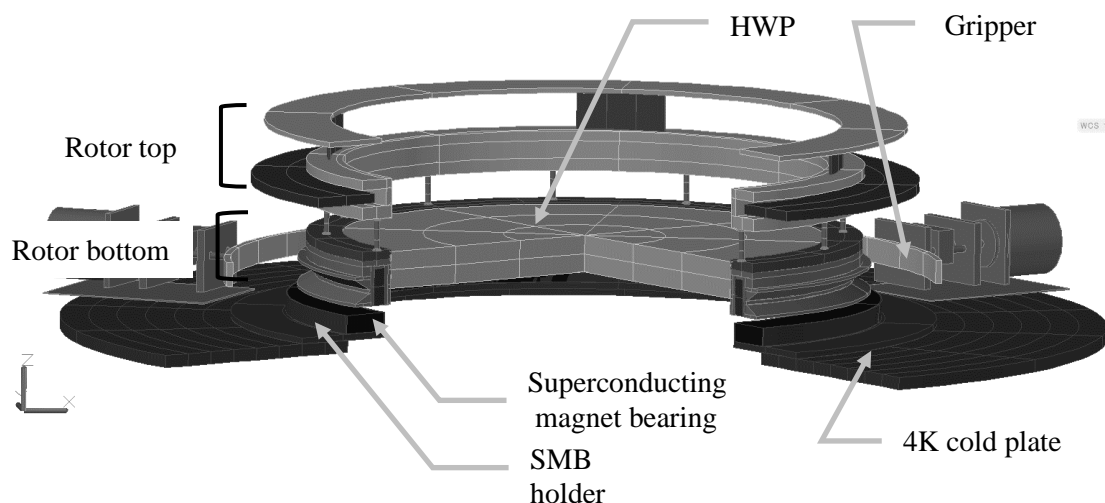


Figure 2. Thermal model of the full-size polarization modulation unit with HWP.

Table 1. Assembly material list

Assembly name	Material	Remarks
Rotor top	Aluminium 6061 ^a , SUS304 ^b	For rotation
Permanent magnet	SmCo ^c	
Rotor bottom	Aluminium 6061	For levitation
HWP	Sapphire ^d	
Permanent magnet	SmCo	
Superconducting magnet bearing	YBCO ^e	For levitation
SMB holder	G10 ^f	
Grippers	Aluminium 6061	The whole system on this plate
4K cold plate	Aluminium 6061	

^a <http://cryogenics.nist.gov/MPropsMAY/material%20properties.htm>

^b <http://cryogenics.nist.gov/MPropsMAY/material%20properties.htm>

^c Self-measuring

^d *Sapphire: Material, Manufacturing, Applications*

^e Self-measuring

^f <http://cryogenics.nist.gov/MPropsMAY/material%20properties.htm>

The thermal properties, thermal conductivity and specific heat, are set as a function of temperature on the model. The surface finish of the most assemblies is a metal colour as aluminium and its infrared emissivity is 0.11 while the surface of YBCO holder is G10 and its emissivity is 0.96. In the simulation model, the initial temperature and radiative thermal boundary are set to the actual experiment data. The thermal simulation model is constructed on AutoCAD 2018 and simulations are conducted using Thermal Desktop ver. 5.8.

3.2 Experimental data for a thermal model

The entire PMU system is placed on the 4 K environment. Experimentally the system is cooled by a 4 K GM cooler. The radiative thermal boundary condition is set to be the shroud temperature experimentally measured.

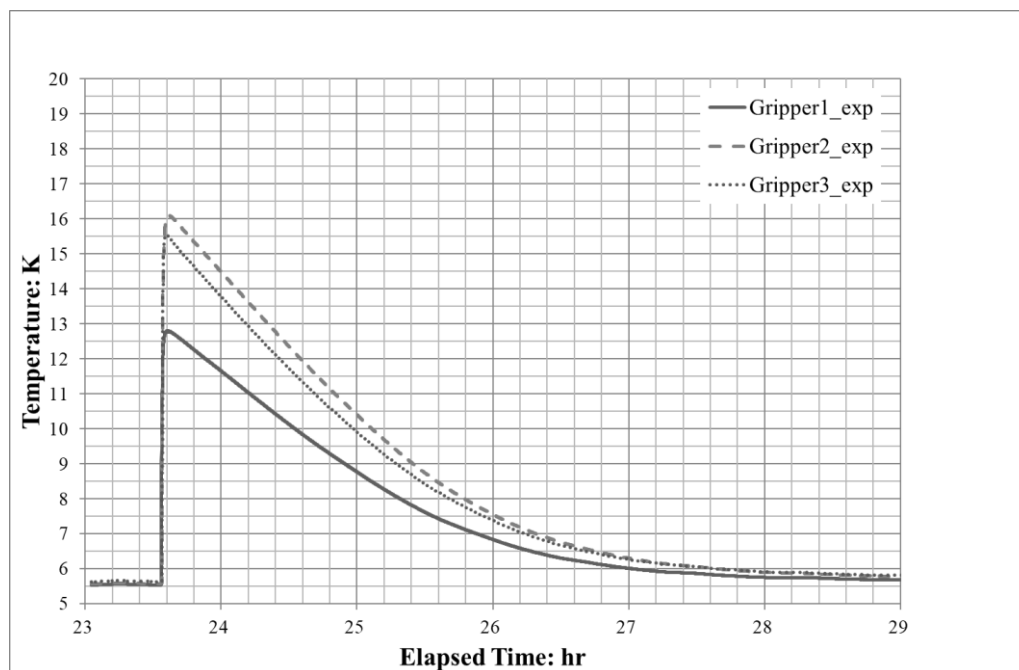


Figure 3. Transient gripper temperature profiles.

We conducted the experiment to acquire the data for the thermal analysis. The rotating speed of rotor is set to be 60 rpm. The rotor is rotated during several tens of hours and then it is stopped and grabbed by the grippers. A temperature sensor, Cernox, is attached on each gripper and the transient temperature profile is measured. Each experimental data is plotted as shown in Figure 3.

The rotor is rotated for almost 24 hours and then stopped. After this, each gripper grabs the rotor almost every 10 sec. At the instant the rotor is grabbed by the first gripper, its temperature suddenly rises because the heat accumulated on the rotor flows into the gripper. Next, the second gripper pushes and grabs the rotor and its temperature rises. The peak of second gripper temperature is larger than the first ones because the first gripper is already in contact with the rotor and it tries to keep the rotor position when the second gripper pushes the rotor to grab. Thus, the thermal contact conductance between the second gripper and the rotor is larger. More heat flows into the second gripper from the rotor. At last the third gripper contacts the rotor. However, the third gripper temperature rise is smaller than the second one because the remaining heat on the rotor is smaller than at the contact with the second gripper. After all grippers grab the rotor, their temperatures very slowly fall back to the initial 4K cold plate temperature. It is noted that the temperature profile of each gripper is different from one another because their thermal contact conductances are different, and that roughly speaking, the heat piled on the rotor is very dependent on the temperature peak of the second gripper. This is the key to correlate the thermal model.

3.3 Comparison of simulation result with experimental result

The experimental and simulation data are plotted together in Figure 4. The rotor temperature is also calculated and shown in the figure. The heat dissipation and three thermal contact conductances are taken as free parameters to fit the experimental temperature profiles. As the estimated value, the heat dissipation on the current rotor is about 10 mW.

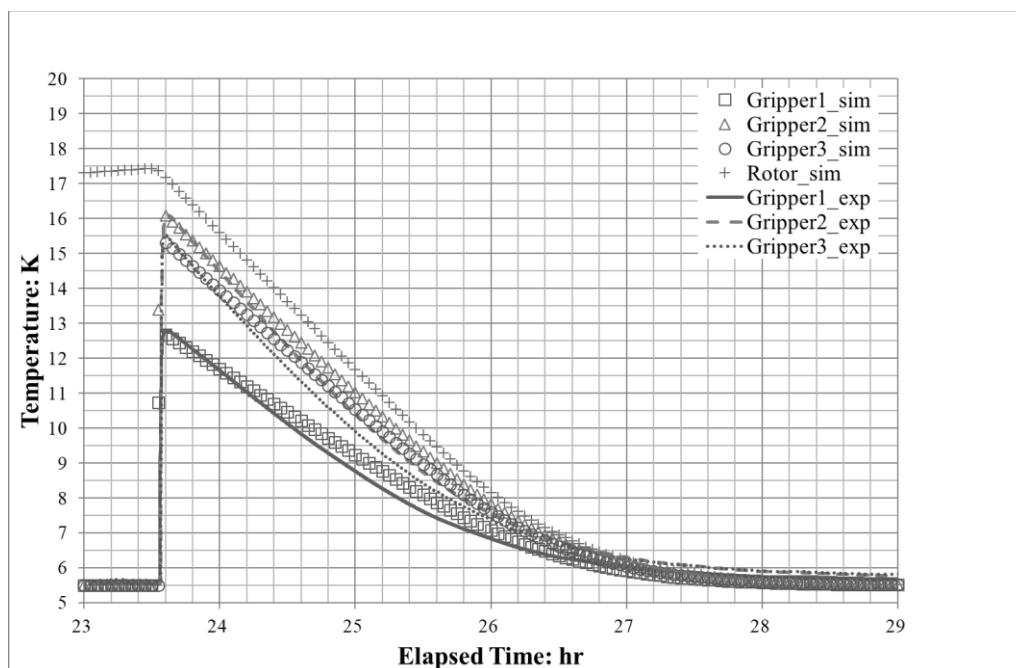


Figure 4. Comparison of an experimental result with a simulation result.

Thermal contact conductance of each gripper at different experimental runs are shown in Table 2. In these experimental runs, all the rotor speeds are the same, 60 rpm. Thus, the heat dissipation on the rotor is also the same. However, a thermal contact conductance of the same gripper is different at each experimental run. Each thermal contact conductance value of G1 and G2 has an especially large

difference at each run because the contact pressure between the rotor and gripper at each run is different and not always the same in such a soft contact condition.

Table 2. Thermal contact conductance each gripper at different experimental runs

Exp. Run	Estimated Heat Dissipation	Estimated Thermal Contact Conductance of Gripper		
	mW	G1 (W/K)	G2 (W/K)	G3 (W/K)
#1	10	0.02	0.12	0.05
#2	10	0.02	0.10	0.05
#3	10	0.01	0.10	0.05
#4	10	0.01	0.19	0.05

4. Simulation results of allowable heat dissipation on rotor

Using the correlated thermal model on which HWP is placed, we estimated the HWP equilibrium temperature in the condition of 60 rpm rotation on the rotor. HWP temperature as a function of heat dissipation on the rotor is calculated with some heat dissipations, as shown in Figure 5. From the point of thermal requirement for the HWP, the equilibrium temperature must be 20 K or lower. Thus, the heat dissipation on the rotor must be lower than about 1.1 mW from the graph.

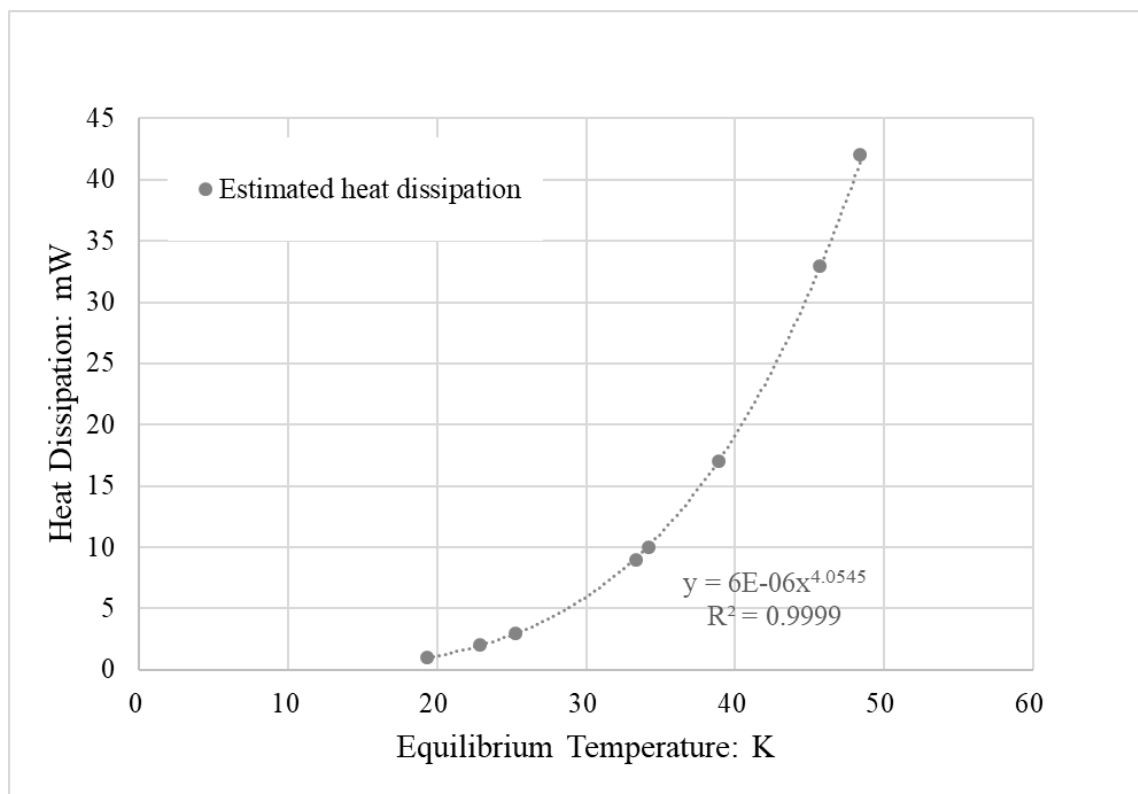


Figure 5. Heat dissipation on the rotor as a function of HWP equilibrium temperature.

5. Conclusions

We have established the thermal structural model of PMU and estimated the heat dissipation to the levitating rotor from its rotation driven by the AC motor. For a model building we rely on the transient temperature profiles of the rotor using the thermometer on each gripper and derive the heat dissipation and the three gripper conductances. Based on this model, the estimated heat dissipation on the current rotor is 10 mW.

The heat dissipation must be 1 mW or smaller to keep the HWP equilibrium temperature lower than 20 K when the HWP is rotating. The current rotor design does have rooms for further optimizations to minimize the heat dissipation. One of them is to suppress the fluctuation in magnetic flux density on the rotor and the YBCO array. The other is to minimize use of metal materials on the rotor or simply to employ a non-metallic material. We will carry out the further optimizations based on this model and report the future paper.

6. References

- [1] Sakurai Y, Matsumura T, Kataza H, Utsunomiya S and Yamamoto R 2017 *IEEE Transactions on Applied Superconductivity* **27** no 4 3601904
- [2] Matsumura T, Sakurai Y, Kataza H, Utsunomiya S and Yamamoto R 2016 *Physica C: Superconductivity and its applications* **530** pp 138-141
- [3] Sakurai Y, Matsumura T, Katayama N, Kanai H and Iida T, 2018 *Proceedings of the 2018 29th IEEE International Symposium on Space Terahertz Technology* **29** pp 170-174
- [4] Sakurai Y, Matsumura T, Sugai H, Imada H, Kataza H, Ohsaki H, Hazumi M, Katayama N, Yamamoto R, Utsunomiya S and Terao Y, 2017 *IOP Conference Series: Materials Science and Engineering* **278** No. 1, p 012011

Acknowledgement

This work was supported by JSPS KAKENHI Grant Numbers JP17H01125 and JP19K14732.